ELSEVIER

Journal of Hydrology 257 (2002) 174–188

Journal of Hydrology

www.elsevier.com/locate/jhydrol

Comparison of alternative modelling approaches for groundwater flow in fractured rock

Jan-Olof Selroos[a], Douglas D. Walker[b,*], Anders Ström[a], Björn Gylling[c], Sven Follin[d]

[a]*Swedish Nuclear Fuel and Waste Management Company (SKB), Stockholm, Sweden*
[b]*Duke Engineering and Services, now at Illinois State Water Survey, 2204 Griffith Dr., Champaign, IL 61820, USA*
[c]*Kemakta Konsult, Stockholm, Sweden*
[d]*Golder Grundteknik, now at SF geologic, Stockholm, Sweden*

Received 9 January 2001; revised 2 August 2001; accepted 12 October 2001

Abstract

In performance assessment studies of radioactive waste disposal in crystalline rocks, one source of uncertainty is the appropriateness of conceptual models of the physical processes contributing to the potential transport of radionuclides. The Alternative Models Project (AMP) evaluates the uncertainty of models of groundwater flow, an uncertainty that arises from alternative conceptualisations of groundwater movement in fractured media. The AMP considers three modelling approaches for simulating flow and advective transport from the waste canisters to the biosphere: Stochastic Continuum, Discrete Fracture Network, and Channel Network. Each approach addresses spatial variability via Monte Carlo simulation, whose realisations are summarised by the statistics of three simplified measures of geosphere performance: travel time, transport resistance (a function of travel distance, flow-wetted surface per volume of rock, and Darcy velocity along a flowpath), and canister flux (Darcy velocity at repository depth). The AMP uses a common reference case defined by a specific model domain, boundary conditions, and layout of a hypothetical repository, with a consistent set of summary statistics to facilitate the comparison of the three approaches. The three modelling approaches predict similar median travel times and median canister fluxes, but dissimilar variability. The three modelling approaches also predict similar values for minimum travel time and maximum canister flux, and predict similar locations for particles exiting the geosphere. The results suggest that the problem specifications (i.e. boundary conditions and gross hydrogeology) constrain the flow modelling, limiting the impact of this conceptual uncertainty on performance assessment.

Keywords: Groundwater; Numerical model; Fractured rock; Waste disposal

1. Introduction

The location, design, and permitting of deep geologic repositories for spent nuclear fuel include performance assessment studies that quantify the risks of the disposal method to society. These performance assessments are integrated site characterisation and modelling studies that examine the features, events, and processes that contribute to repository performance. One of the main scenarios studied is potential transport of radionuclides from defective canisters in the repository to the accessible environment (Skaguis et al., 1996; SKB, 1999). The radionuclide transport is primarily governed by groundwater flow and various mass transfer phenomena. Uncertainties regarding site characteristics and process models are inherent to

* Corresponding author. Tel.: +1-2173331724; fax: +1-2172440777.
E-mail address: ddwalker@uiuc.edu (D.D. Walker).

0022-1694/02/$ - see front matter
PII: S0022-1694(01)00551-0

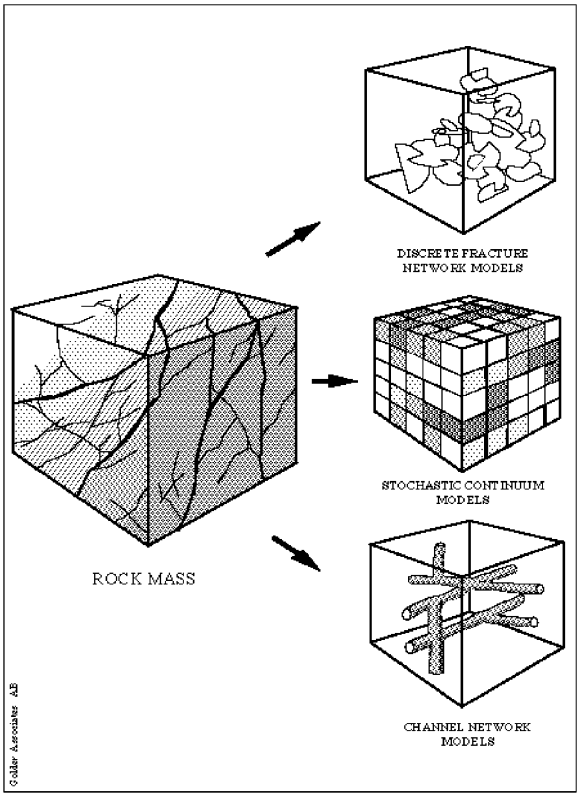

Fig. 1. Alternative geometrical conceptualisations of the fractured rock considered in this study for groundwater flow and solute transport.

performance assessment studies, and may affect conclusions regarding repository safety. One approach to addressing uncertainties of process models is to apply alternative modelling approaches to the same site, then compare the results to evaluate the impacts of the uncertainty.

The Alternative Models Project (AMP) is a comparative uncertainty analysis conducted by the Swedish Nuclear Fuel and Waste Management Company (SKB) as part of the SR 97 project (SKB, 1999). SR 97 is a comprehensive performance assessment of three hypothetical repositories for nuclear waste disposal, located at real sites in Sweden. During the course of SR 97, scientists and engineers debated the uncertainty and limitations of adopting any single approach to modelling the groundwater flow process. The chief concern of this debate was if alternative conceptualisations of groundwater movement in fractured media might lead to differences in simulated groundwater velocities that would in turn, affect the conclusions of the performance assessments. To resolve this debate, SKB commissioned the AMP study which compares three alternative approaches for modelling groundwater flow: Stochastic Continuum (SC), Discrete Fracture Network (DFN), and Channel Network (Fig. 1). The AMP applies all three approaches to the same site and compares their results to evaluate the impacts of using alternative approaches to groundwater flow modelling in fractured rock.

The specific objectives of the AMP are to (1) illustrate the impacts of using alternative approaches for modelling groundwater flow and advective transport in fractured rock; and (2) determine the appropriateness of using a single approach to groundwater flow modelling in a performance assessment for nuclear waste disposal. The AMP by itself is not a performance assessment, but rather is a comparison of alternative approaches to modelling groundwater flow. Thus, the AMP compares the results of groundwater flow models that are relevant to performance assessment, but the AMP does not explicitly model the waste canisters, nor does it calculate the radionuclide dose. The reader should note that the site of the hypothetical repository is real, and, although thoroughly characterized, the true performance of any repository at the site remains unknown. The AMP consequently does not examine the potential biases of the site characterisation or the alternative models, only the relative differences between model results.

Three separate modelling teams were selected to participate in the AMP (Dershowitz et al., 1999; Gylling et al., 1999a,b; Widén and Walker, 1999), each experienced in the use of their models and familiar with the site hydrogeology. The problem premises and the compilation of results are explicitly specified so that the comparison will illustrate the impacts of alternative modelling approaches rather than the impacts of different hydrogeologic interpretations. The modelling teams were allowed some latitude in inferring model parameters from the data, since these are viewed as being inherent to each conceptual model. The teams were free to select simulation options such as grid densities, convergence tolerance, the number of realisations, etc. since these are viewed as being model and application specific. This paper

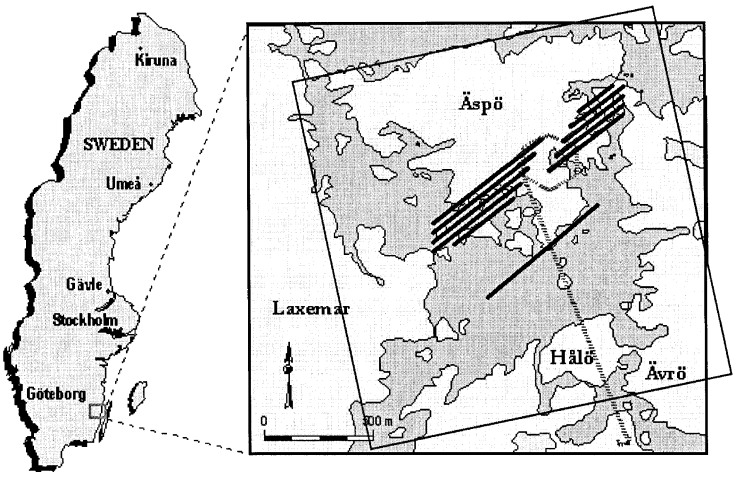

Fig. 2. The study site location, showing the Äspö Hard Rock Laboratory (dashed line), the site-scale modelling domain (square) and the canisters of the hypothetical repository (heavy lines).

consequently describes the application of each approach in detail, emphasising parameter choices and modelling decisions believed to lead to differences in the results. References are cited for readers interested in the numerical methods used by each approach.

2. The AMP comparison

2.1. Site description

The hypothetical repository is sited at Äspö, an island just off the southern Swedish coast in the Baltic Sea (Fig. 2). Äspö is also the location of the Äspö Hard Rock Laboratory, an underground research facility owned and operated by SKB. The characterisation studies of the Äspö site include surface, borehole, and tunnel investigations (Rhén et al., 1997; Walker et al., 2001). Thin soils overlie crystalline bedrock (Småland granite), and the region experiences isostatic rebound from continental glaciation (approximately 1.5 mm/yr). Fresh groundwater near the surface rests on low-salinity water that has intruded from the Baltic Sea. Regional numerical models of Äspö (Rhén et al., 1997; Svensson, 1997) indicate that a small net infiltration onshore combines with land surface variations such that flow paths are largely upward from the repository to the shallow waterways surrounding the island. This is consistent with the site geochemistry, which indicates that relatively old groundwater flows upward through the repository, mixing with young precipitation, and exiting to the Baltic Sea.

Rhén et al. (1997) describe 18 fracture zones over 500 m in length that fall within the modelling domain, fully penetrating the domain from top to bottom (Fig. 3). These zones are referred to as the site-scale conductor domain, with transmisssivities specified for each zone based on cross-borehole interference tests. The remainder of the modelled domain is referred to as the site-scale rock domain, which has several sub-units with distinct hydraulic conductivities. Based on interpretations of packer tests, Andersson et al. (1998) estimated the flow-wetted surface area per volume of rock as $a_r = 1.0\ m^2/m^3$ rock, and the flow (or kinematic) porosity as $\varepsilon_f = 1 \times 10^{-4}$, both assumed uniform throughout the domain.

The hypothetical repository is derived from a design specific to the Äspö site (Munier et al., 1997) that maintains a 100 m distance between repository tunnels and major fracture zones, and a 50 m distance between tunnels and smaller zones. To reduce the computational burden, the AMP uses just three blocks of the repository design, all at the 500 m level. These blocks are chosen to represent different rock conditions and capture the discharge areas of solutes transported from the repository. The resulting repository

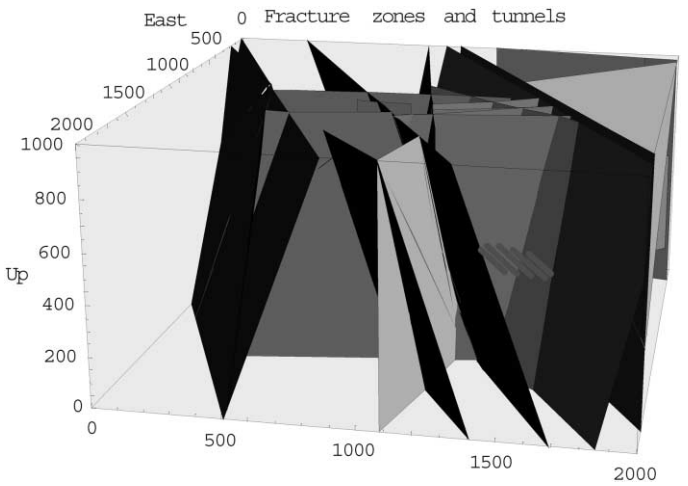

Fig. 3. The Site-scale Conductor Domain fracture zones within the site model domain, as seen in elevation view from the east. The heavy lines are the locations of some of the repository tunnels. All numbers in metres.

contains 945 canisters in 11 tunnels, with canisters spaced every 6 m within the tunnels (note that the only use of the canisters in the AMP is to locate particle starting positions—the canisters themselves are modelled by a separate process model in SR 97 performance assessments).

2.2. Study specifications and restrictions

The AMP comparison is intended to illustrate the differences between different conceptualisations of groundwater movement in fractured rock, and to this end explicitly specifies the problem premises and data. The modelling teams were restricted to the data available in SKB reports and the SKB SICADA database, which catalogues the hydraulic test results, fracture mapping, tracer tests, and other information previously gathered at the Äspö site. The modelling teams were also required to document all data use and parameter inference. Thus, although the type and degree of data utilisation depends on the modelling approach, no new field investigations are conducted for the AMP so that the model applications are based on essentially the same data. The modelling applications all use the same deterministic geologic structural model for fracture zones and fracture zone transmissivities provided by Rhén et al. (1997) (Fig. 3). Each of the approaches is applied to a common site-scale model domain, defined as a volume 2000×2000 m^2 of horizontal extent, and 1000 m in depth, with the upper surface of the model at the Baltic Sea level (Fig. 2). The applications all use stochastic descriptions of the heterogeneous rock properties, with Monte Carlo simulations providing probability distributions of groundwater velocities, flow paths, and advective travel times from representative canister positions. The AMP study uses a nested modelling approach (Ward et al., 1987), with constant head boundary conditions for the site-scale models derived from the freshwater heads of a single realisation of the heterogeneous regional groundwater model of Svensson (1997). The total flow estimated by the regional model across each face of the site-scale domain provides a check on model consistency and mass balance.

As described earlier, the modelling teams are constrained to a single interpretation of the site, a well-defined domain, a controlled data set, and specific values of key parameters. However, some leeway in interpreting the data, inference, and implementation of various parameters must be allowed so that each approach actually represents an alternative conceptualisation of the site heterogeneity. Thus, the AMP is forced to allow deviations from the problem premises if they can be defended as being inherent to the modelling approach.

The modelling results are summarised by the statistics of three simplified measures relevant to repository performance. The first of these measures is the

Table 1
Summary of model applications within the AMP (the character σ denotes the standard deviation of the distribution)

	Stochastic continuum	Discrete fracture network	Channel network
Deterministic zones	● Mean K and variance by zone, up-scaled from interference tests	● T from interference tests	● Conductance mean and variance by zone, up-scaled from interference tests
	● $\sigma_{\log_{10} K} = 1.6$ ● Integral scale = 32 m	● Homogeneous within zone	● $\sigma_{\log_{10} C} = 0.8$
Rock mass/non-zone	● Mean K by region, up-scaled from 3 m packer test ● Log-normal with mean K between 1×10^{-8} and 1×10^{-7} m/s, $\sigma_{\log_{10} K} = 1.6$ ● Integral scale = 32 m	● Log-normal radius with mean 6 m, $\sigma_R = 3$ m, $0.2 < R < 20$ m ● Log-normal Radius with mean 14 m, $\sigma_R = 13$ m, $20 < R < 1000$ m ● Log-normal T with mean 9×10^{-7}, $\sigma_T = 5 \times 10^{-6}$, min 1×10^{-9}	● Mean conductance up-scaled from 3 m packer test ● Log-normal with mean = 6×10^{-9} m/s, $\sigma_{\log_{10} C} = 0.8$
Flow-wetted surface	Homogeneous, 1.2 m^2/m^3 rock	Calculated for each fracture as area exposed to flow	● Zones: 1.2 m^2/m^3 rock ● Rock: 0.12 m^2/m^3 rock ● EDZ: 0.04 m^2/m^3 rock
Repository/realisations	● 945 cans × 34 realisations ● EDZ below scale of resolution	● 50–90% of 81 cans × 10 realisations ● EDZ as canister fractures, $T = 1 \times 10^{-9}$	● 229 cans × 30 realisations, taking median of 200 particles ● EDZ has 10 × conductance of rock mass

canister flux, q_w, calculated as the flow of groundwater per unit area at each representative canister position (i.e. the Darcy velocity). Another measure is the advective travel time, t_w, from representative canister locations to the discharge surface. Note that the advective travel time is an intermediate product of the groundwater flow model, rather than a purely physical entity. The actual transit times of solutes and water from repository depth to the discharge surface are also affected by diffusion into the stagnant water of the rock matrix. Matrix diffusion implies considerably longer transit times than indicated by the advective travel times alone. The last measure is the F-quotient (yr/m), or transport resistance, defined for a single fracture as:

$$F = \frac{2LW}{Q} \tag{1}$$

and for a porous medium with constant Darcy velocity, homogeneous flow-wetted surface and porosity as

$$F = \frac{d_w a_r}{q_w} = t_w a_w \tag{2}$$

where L is the length travelled within the fracture (m), W is the fracture width wetted by flowing water (m), Q is the flow rate in the fracture (m^3/yr), d_w is the advective travel distance (m), q_w is the Darcy velocity (m/yr), a_r is the flow-wetted surface per rock volume (m^{-1}), t_w is the advective travel time (yr), and a_w is the flow-wetted surface per volume of water (m^{-1}). The F-quotient is useful in evaluating flow models since it incorporates the potential for rock interaction, i.e. matrix diffusion and also subsequent sorption in the matrix for reactive solutes (SKI, 1997). The F-quotient is integrated along pathlines in the spatially variable case (i.e. spatial variability in Darcy velocity and/or flow-wetted surface), but is simply a re-scaled travel time if the porosity and flow-wetted surface are homogeneous (Andersson et al., 1998). These three simplified measures—the advective travel time, the canister flux, and the F-quotient—are relevant because they are the main results of the groundwater flow model used in subsequent calculations of the SR 97 performance assessments. Consequently, the impacts on performance assessment of alternative approaches to groundwater flow modelling can be judged by comparing these simplified measures.

The AMP study compares expected behaviour and

variability of the performance measures to assess possible systematic bias and the range or spread of the predicted measures. The comparisons are based on the statistics of travel time, canister flux, and *F*-quotient averaged over all canisters, which are sorted into various sets (e.g. for the ensemble (pooled) over all realisations and canisters, and for single realisations). The statistics include the sample arithmetic mean and variance (as estimators of the true mean and true variance); the sample median, 5th, and 95th percentiles; and the 'spread' of the sample (i.e. absolute difference between the 5th and 95th percentiles). The performance measure distributions have a wide range and are positively skewed, thus the statistics are calculated for the common logarithms of the performance measures.

3. Alternative approaches to modelling flow in fractured rocks

Modelling groundwater flow in fractured rocks is relatively complex because the fractures can be as difficult to observe and characterise as they are to represent in a numerical model. Alternative modelling approaches infer properties, represent fractures, and resolve scale dependencies in various ways. Fig. 1 shows the conceptual approaches considered in the AMP: (1) a Stochastic Continuum model (HYDRASTAR); (2) a Discrete Fracture Network model (FracMan/PAWorks); and (3) a Channel Network model (CHAN3D). Although each approach has been applied successfully to field-scale experiments in fractured rocks at Äspö (Walker et al., 1996; Uchida et al., 1994; Gylling et al., 1994, 1998), the AMP evaluates these alternative conceptual models in terms of differences in their results that could affect the performance assessment. Section 3.1 summarises the application of each approach, with an emphasis on features thought to lead to differences in results. Table 1 summarises each of the applications.

3.1. Stochastic continuum model

SC modelling of groundwater flow in fractured rocks assumes that, over some representative volume, the fractured rocks may be represented as an equivalent homogeneous porous medium with groundwater flow governed by Darcy's law. The hydraulic conductivity of the equivalent system is treated as a random spatial distribution of block/element hydraulic conductivities that represent the spatially averaged fracture properties. For the AMP, Widén and Walker (1999) used HYDRASTAR, a stochastic continuum modelling code developed by SKB (SKB, 1992). HYDRASTAR simulates log-normally distributed, heterogeneous hydraulic conductivity fields, incorporating deterministic conductive fracture zones as explicit regions of increased mean conductivity. A node centred finite-difference numerical approach solves the governing equations for three-dimensional groundwater flow within the simulated conductivity fields, followed by advective particle tracking from each canister position. The simulation of hydraulic conductivity, flow solution, and particle tracking is repeated in Monte Carlo fashion to develop probability distributions for the travel paths and arrival times (Neuman, 1988; Norman, 1992).

The HYDRASTAR application for the AMP consists of a three-dimensional, uniform 25-m grid, with prescribed head boundary conditions adapted from the regional model by simple linear interpolation. The measured hydraulic conductivities are adjusted (up-scaled) from the measured to the block scale using an empirical relationship developed by Rhén et al. (1997) from Äspö packer test data

$$\log_{10} K_{gu} = \log_{10} K_{gm} + 0.782(\log_{10} L_u - \log_{10} L_m) \quad (3)$$

where K_g is the geometric mean of hydraulic conductivity (m/s), and L is the length scale (m), assumed equal to the packer interval. The subscripts m and u refer to the measurement and up-scaled values, respectively. Interference tests in the fracture zones are used to infer the conductivities of the fracture zones in the conductor domain, and the 3-m packer tests are used to infer the conductivities of the rock domain. The rock domain and conductor domain are explicitly specified as deterministic step changes in the geometric mean of block conductivities.

HYDRASTAR's geostatistical simulation algorithm is limited to a single variogram model throughout the domain, inferred in this application from the 3-m tests in the rock domain. This inference first regularises the hydraulic conductivities from the 3-m packer tests via the arithmetic mean of 3-m packer

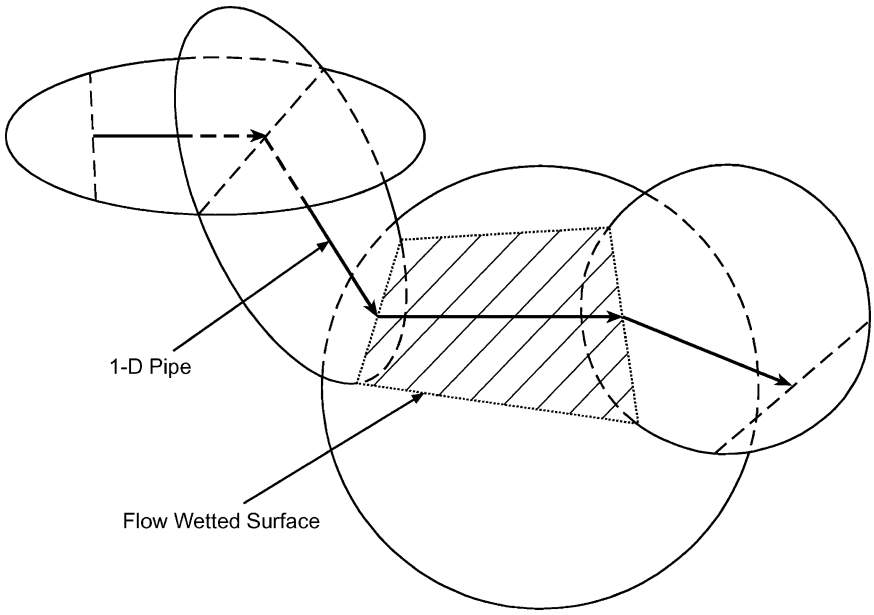

Fig. 4. Discrete Fracture Network (DFN) conceptual model.

tests within a 25-m moving window, multiplied by a correction factor to account for packer length and borehole radius (see Norman, 1992). The common logarithms of these conductivities (now regularised to the 25-m scale) are fitted with a model variogram via Iterative Generalized Least Squares Estimation (Neuman and Jacobsen, 1984; Walker et al., 2001). This regularisation-and-variogram-fitting suggested that, to simulate log conductivities for the 25-m blocks, an appropriate variogram model is an isotropic, exponential model with a practical range of 97 m (integral scale of 32 m), zero nugget, and variance of 2.72. HYDRASTAR cannot represent spatially variable porosity or flow-wetted surface, thus this application uses a homogeneous flow porosity of $\varepsilon_f = 1 \times 10^{-4}$, and a homogeneous flow-wetted surface of $a_r = 1.2\ m^2/m^3$ rock. These are used as scaling factors to determine the travel time and *F*-quotient from the Darcy velocity (Eq. (2)).

The SC model application includes all 945 canisters of the hypothetical repository (i.e. 945 particle starting points per realisation). The excavation-disturbed zone around each repository tunnel is not included, since the block dimensions of this grid are too large (25 m) to resolve the narrow thickness of the excavation-disturbed zone (0.3–1.0 m). A brief stability analysis indicates that the median performance measures are approximately stable after 20 realisations; 34 realisations are used (the maximum that could be managed by the post-processing software). Widén and Walker (1999) provide additional details of this model application.

3.2. Discrete fracture network

DFN models are based on the premise that groundwater flow and transport in crystalline rocks occur primarily within fractures. Thus, this approach simulates individual fractures in the rock, then solves for the flow and transport in the interconnected fracture system (Fig. 4). The AMP uses FracMan/FracWorks and PAWorks for the DFN approach (Dershowitz et al., 1999), generating stochastic fractures with properties inferred from the reference site data. The resulting fracture networks are converted to three-dimensional networks of one-dimensional pipes with properties equivalent to each fracture in the network. Boundary conditions are assigned and a finite element method solves for flow within the pipe network. For a representative percentage of the repository canisters, a graph-theory search algorithm identifies, characterises, and

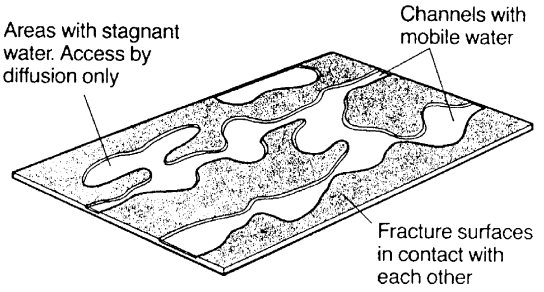

Fig. 5. Channel Network (CN) conceptual model of a fracture plane.

follows pathways from the canisters to the discharge areas.

This application of DFN uses three nested levels of resolution to represent the fractures in the model domain. The greatest resolution was specified near the repository, including 99.7% of the fractures (only omitting fractures smaller than 0.2-m radius). The distribution of this detailed set is inferred from fracture statistics gathered in the bored tunnel (Follin and Hermansson, 1996). The second level of resolution covers the entire domain with fractures of radius >20 m, inferred from observed fracture statistics (Uchida and Geier, 1992; Uchida et al., 1994). The lowest level of resolution is the 18 fracture zones of the conductor domain, which are included in each realisation with geometries and homogeneous transmissivities as prescribed for use in the AMP study (Fig. 3). This nested representation realistically connects the canister emplacement boreholes to the surrounding fracture zones, while preserving the correct hydraulic gradient through the repository area and minimizing the computational demand (Dershowitz et al., 1999). The parameters of fractures >20 m radius could be calibrated so that the boundary flows of this site-scale model would match the flows estimated by the regional model (T. Doe, personal comm., 1999), but calibration is not permitted by the AMP premises, and thus some discrepancy between the boundary flows is possible for this application.

Based on trace maps in a bored tunnel at the Äspö site, it has been found that 37% of mapped fractures terminate at intersections with other fractures (Follin and Hermansson, 1996). This is incorporated into the DFN model by using the BART (Enhanced Baecher) spatial location conceptual model (Dershowitz et al., 1989), which explicitly accounts for the fracture connectivity pattern. Borehole data from a tracer test site at Äspö supports the chosen spatial model (Dershowitz et al., 1996). The fracture orientations are modelled via a bootstrap approach (Dershowitz et al., 1996), matching the simulated orientations to those measured in the bored tunnel. The conductive fracture intensity and the fracture transmissivity distribution are derived from packer testing in the rock domain (Uchida et al., 1997). The fracture transport aperture is set to $\alpha = 0.5T^{1/2}$, a relation shown to be successful in predictions and transport simulations (Uchida et al., 1994). The flow-wetted surface is not explicitly defined, but is calculated for each fracture as the path area exposed to flow and consequently is spatially variable (Fig. 4).

This application defines the pathway source as the canister emplacement holes, and the sink is defined by the discharge surface of the model. The branch option of PAWorks generates a high number of similar pathways due to the high connectivity near the repository and lower connectivity in the surrounding domain. To limit the computational burden, this application analyses only the main branch with the highest flow rate and neglects mixing at intersections. Defining path priority by the highest flow rate is known to provide results similar to those of simple particle tracking, which was judged sufficient for this application.

To reduce the computational demand, this application considers only 81 representative canisters of the hypothetical repository. Not all regions of the model are connected to flowing fractures in every realisation, thus only 50–90% of the canisters are connected to flow in any individual realisation. That is, 50–90% of 81 representative canister positions are included in the pathway analysis of any realisation. The excavation-disturbed zone around each repository tunnel is not included, except for a box-like fracture set that represents the canister deposition holes. The 10 realisations are chosen by experience to be sufficient for this application (Dershowitz et al., 1999).

3.3. Channel network model

Field observations suggest that fracture surfaces are uneven and mineralised, such that flow and contaminants are distributed non-uniformly across the fracture

plane in preferential paths, or channels (Fig. 5). These channels may intersect in three-dimensional space, forming a network of channels for the movement and mixing of flowing water (Neretnieks, 1993). Moreno and Neretnieks (1993), Moreno et al. (1997) and Gylling (1997) represented this network with stochastic conductance values arranged on a rectangular grid, conceptually representing the channels as discrete, one-dimensional flow paths intersecting in three-dimensional space. The resulting Channel Network model, CHAN3D, solves for flow in each channel of the system via the finite-difference method. While the flow formulation of CHAN3D is similar to the finite-difference grid solution used in HYDRASTAR, CHAN3D allows including additional nodal connections to represent deterministic features, such as tunnels. CHAN3D uses a 'total mixing approximation' at channel intersections, releasing multiple particles at each starting point that randomly disperse at intersections assuming a flow-weighted probability of entering a channel. CHAN3D can represent additional interactions with the rock (e.g. sorption), but these are not allowed under the AMP problem premises (Gylling et al., 1999b).

Gylling et al. (1999a) applied the Channel Network approach to the hypothetical repository, using an effective channel length (grid spacing) of 30 m. Both the conductor and rock domain are represented, inferring parameters from water injection tests in individual boreholes (measurements in the tunnels are excluded from the inference of this application due to uncertainties associated with tunnelling damage). Channel conductances are represented using effective values to represent channels smaller than the 30-m effective channel length. For this application, moving window statistics are used to evaluate the scale dependence on the mean and standard deviation of the log conductance distributions. Channel conductances in the conductor domain are inferred from the prescribed fracture zone transmissivities using moving-window statistics in simulated fields, concluding that the fracture zone conductivity is scale-dependent. This moving window approach also infers up-scaling factors for the mean log conductance of each fracture zone in the conductor domain. Based on fracture frequencies and packer test data, the estimated flow-wetted surface area is 1.2 $m^2/(m^3$ rock) for all zones in the conductor domain. A moving average of 3-m packer tests within a 30-m window is used to estimate up-scaling factors for the rock domain mean log conductance. This reduces the log conductance standard deviation from 1.5 to 0.8, for the rock domain; the same variance was used for the log conductance of the conductor domain. The spatial correlation of log conductance is omitted in this application since the inferred spatial covariance has a short integral scale (short range and high nugget) and thus is judged to have little influence. This application uses a single rock domain (i.e. no sub-units), with one-tenth of the flow-wetted surface value of the conductor domain.

Channels falling within the excavation-disturbed zone are given a conductance 10 times higher than the mean for the rock mass. The local conductance conservatively assumes the fracture zone value where fracture zones intersect the excavation-disturbed zone. The flow-wetted surface area of the excavation-disturbed zone is estimated to be 0.3 of the conductor domain value. This application includes 229 canisters of the hypothetical repository (i.e. 229 starting locations per realisation). In each realisation, the total mixing approximation releases 200 particles at each starting location to allow calculating the mixing at channel intersections. The median travel time over all particles released at each starting location approximates the median travel time for each canister. Note that the canister flux statistics are unaffected by this approximation, since the canister flux at a given location is constant in a realisation. Based on experience, 30 realisations are used for this application (Gylling et al., 1999a).

4. Results

The results of the AMP site models are similar, with the predicted exit locations discharging into the sea south and east of Äspö Island in all models. This indicates a consistent flow pattern among the models and demonstrates the dominating effect of the boundary conditions and the fracture zones in the conductor domain. Since the AMP premises specify the transmissivities of the fracture zones, it is reasonable to anticipate that the expected performance measures of all three approaches might be similar. On the other hand, the boundary flows across each face of

Table 2
Water flow through the site scale model boundary (positive values indicate flow into the model; values in parentheses are the ratio of regional to site-scale flow)

Model surface	Regional (l/s)	Stochastic continuum (l/s)	Channel network (l/s)	Discrete fracture network (l/s)
West	+10.3	6.99 (1.47)	12.05 (0.86)	0.70 (14.71)
East	−0.354	−0.953 (0.37)	−0.74 (0.48)	0.07 (−5.06)
South	0.444	6.5 (0.068)	1.84 (0.24)	0.09 (4.93)
North	−0.972	−0.0379 (25.65)	−1.86 (0.52)	0.50 (−1.94)
Bottom	1.22	−0.0962 (12.68)	1.13 (1.09)	0.30 (4.07)
Top	−10.7	−12.3 (0.87)	−12.43 (1.09)	−1.66 (6.45)
Total inflow	11.96	13.5 (0.89)	15.02 (0.80)	1.66 (7.20)
Total outflow	−12.026	−13.4 (0.90)	−15.03 (0.80)	−1.66 (7.25)
Mass balance	−0.062	0.103	−0.01	0.00

the site-scale model domain show some discrepancies (Table 2), even though the steady-state mass balance indicates an error of less than one percent for all the models. The Channel Network and SC applications have boundary flows similar to each other and to the regional model (Table 2), but the DFN application under predicts the boundary flows. This suggests that, although the flow patterns and major conductors of each model application are similar, we also should anticipate differences in the results.

It is also important to note the differences between the applications of each model (Table 1) that might effect the estimated moments of the performance measures. The SC modelling study found that approximately 20 Monte Carlo realisations are needed for stable estimates of the median performance measures, and then uses slightly more realisations (34) of all 945 canisters. The Channel Network modelling study uses 30 realisations of only 24% of the canisters, and averages the results from multiple particle releases at each canister in order to obtain a single travel time and *F*-quotient estimate for each canister. The DFN modelling study uses 10 realisations and considers just 9% of the canisters, many of which are not connected to the fracture network in a given realisation. In contrast to Dershowitz et al. (1999), which presented the DFN study results for the three repository blocks separately, the results of Dershowitz et al. (1999) are aggregated and recompiled for this paper.

The Monte Carlo stability of the SC application suggests that the estimates of the lower-order moments (mean and median) are stable, but it is possible that higher-order moments (variance and extreme quantiles) may not have stabilized. The Channel Network application uses experience rather than a Monte Carlo stability analysis to determine the number of realisations, thus the stability of the estimators must be assessed indirectly by comparison to the SC application. The similar finite-difference grid resolutions of the SC and Channel Network applications suggest that the methods are comparable. The low standard deviation of log conductance in the Channel Network suggests that, because the SC standard deviation of log conductivity is higher, the medians of the Channel Network model are also stable. The DFN application also uses experience to evaluate the number of realisations, and does not evaluate the Monte Carlo stability of the estimates. Informal jack-knife analysis of the DFN estimates suggests that its median performance measures are stable relative to the differences between the medians of the alternative approaches. For all three approaches, it is possible that the Monte Carlo estimates of the higher-order moments will not have stabilised. Consequently, although the median performance measures of all three approaches are arguably stable, the variances and extreme quantiles should be viewed cautiously.

4.1. Expected performance measures

Fig. 6 presents the median performance measures as solid squares (Table A2 presents the full set of statistics). Except for the *F*-quotient, the alternative modelling approaches yield similar median results (e.g. the median travel times are between 10 and 30 yr), and the median canister fluxes are between 5.5×10^{-4} and 3.0×10^{-3} m/yr. The similarity of

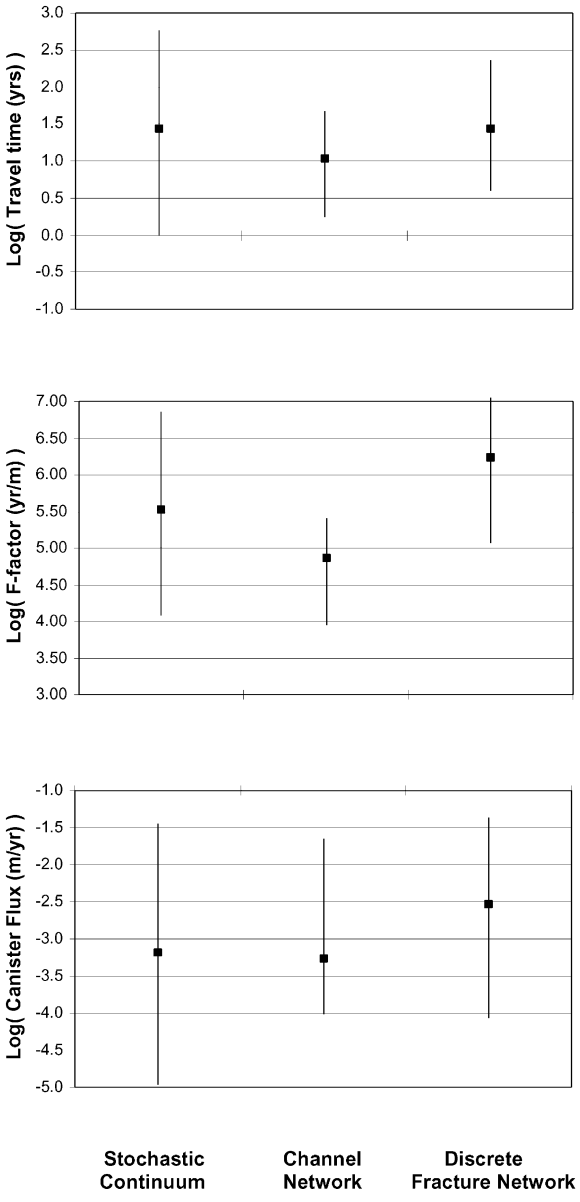

Fig. 6. Performance measures for the three alternative approaches to the hypothetical repository. Median (squares) and range as 5th and 95th percentiles (whisker).

the median results contrasts with the boundary flow discrepancies given in Table 2, where the total inflows of the DFN model are an order of magnitude lower than the other approaches. However, all of the applications include the deterministic fracture zones of the Conductor Domain, and the transmissivity values of these structures are the same in all three applications (i.e. the AMP premises do not allow calibration). The overall gradient, the presence of these features, and the specification of their mean transmissivities in all models apparently determine the median results. This suggests that the AMP premises of boundary conditions, major conductors, and the conductivity data control the results of all three models.

Fig. 6 also indicates that the median travel times of both the SC and DFN models are approximately the same, but that the DFN model yields the greater median F-quotient. This difference is attributed to the different methods for incorporating the flow-wetted surface in the three alternative model applications. The SC application calculates the F-quotient as the product of travel time and a constant flow-wetted surface (Eq. (2)). In contrast, the DFN application explicitly calculates the flow-wetted surface for each fracture, so that the flow-wetted surface is spatially variable. The F-quotient is then calculated along each travel path, accumulating this variability. To compare the flow-wetted surface in the different models, we estimate a model-average flow-wetted surface per volume of water using Eq. (2) as $a_w = F/t_w$ [m^2/m^3]. The SC application uses a homogeneous porosity and flow-wetted surface per volume of rock, so $a_w = a_r/\varepsilon_f = 1.2 \times 10^{-4} = 1.2 \times 10^4$ m^2/m^3 water for each pathline. The calculation of a_w is more complex for the DFN, since the flow-wetted surface varies with fracture size, the location of the fracture connection, and the fracture aperture (Andersson et al., 1998). However, using the ensemble averages of F-quotient and t_w for the DFN application (Appendix A), we can estimate $a_w = 5.5 \times 10^4$ m^2/m^3 water (i.e. about half an order of magnitude larger than that of the SC model). A similar calculation for the Channel Network results yields $a_w = 6.9 \times 10^3$ m^2/m^3 water, lower than that of the SC application because the Channel Network application uses lower a_r values in the rock domain and excavation-disturbed zone (see Section 3.3). Thus, the three modelling studies yield similar median performance measures, with the difference in median F-quotients explained by differences in the representations of the flow-wetted surface.

The mean F-quotient of approximately 3×10^5 yr/m and advective travel time of 25 yr for the SC application (Table A1 of the Appendix A) implies

a transit time of over 1500 yr for a water molecule when assuming realistic matrix properties (SKB, 1999). This demonstrates that the model-calculated advective travel times are compatible with observations of very old water at repository depth.

4.2. Variability

Fig. 6 also presents the performance measure variability, with the 'whiskers' showing the 5th and 95th percentiles of the travel time, canister flux, and *F*-quotient. The results indicate that the SC application has the largest spread for all performance measures (see also the variances in Appendix A). The Channel Network application has a lower spread, which may be a consequence of the smoothing introduced by taking the median of 200 particles released at each canister (see Section 3.3). However, the canister fluxes of the Channel Network model are unaffected by this smoothing (there is only one canister flux value per location per realisation). The relatively low canister flux variability reflects the relatively low standard deviation of conductances in the Channel Network application, approximately one-half the standard deviation used in the SC study (i.e. the Channel Network application simply infers and uses a lower spatial variability).

The SC application has a log *F*-quotient spread equal to that of its log travel time, a consequence of using a homogeneous flow-wetted surface (Eq. (2)). The Channel Network application has a spread in log *F*-quotient similar to that of its log travel time, suggesting that, even though this application uses different flow-wetted surface values for each domain, most of the travelled length resides in the conductor domain, whose homogeneous flow-wetted surface adds little variability to the *F*-quotient results. In contrast, the log *F*-quotient spread of the DFN application is greater than that of its log travel time spread, attributed to using a spatially variable flow-wetted surface area (Eq. (1)). Taken together, the relative variability of the AMP models suggests that a spatially variable flow-wetted surface might have important effects on the subsequent radionuclide transport calculations within performance assessment applications.

4.3. Ergodicity

Only the SC application checks the stability of the Monte Carlo statistics, finding that the 34 realisations yield reliable estimates of lower order moments (e.g. the medians). A related issue is the variability seen in each individual realisation, which is a measure of the level of ergodicity. Ergodicity is said to prevail if space and ensemble averages can be interchanged (i.e. if the full variability of the ensemble is seen in every single realisation). If this is the case, only a single realisation is needed to compute the desired performance measures. Since the repository layout in the current study constitutes a fairly large distributed source, it is anticipated that much of the variability is sampled in each realization.

Table A2 of Appendix A lists the estimated variances and uncertainty measures of the single-realisation performance measures (e.g. the variance of the mean travel time, calculated as the variance over all realisations of the mean travel time of individual realisations). The DFN application consistently yields the highest variance and uncertainty estimates, and the Channel Network application consistently yields the lowest (with the exceptions of travel time variance and travel time spread, where the SC application yields marginally higher estimates). This suggests that the Channel Network application is the most ergodic and the Discrete Fracture application generally is least ergodic. However, the estimates of the Discrete Fracture application may be unstable due to limited number of realisations and canisters. The relatively high level of ergodicity seen in the Channel Network application is also demonstrated by the low canister flux variance (Table A1 of the Appendix A), suggesting that the Channel Network application simply has the lowest inferred spatial variability. The fairly high similarity between realizations (as quantified through the variances in Table A2 of the Appendix A) for the SC and Channel Network applications further indicate that an increased number of realizations would not dramatically affect the resulting performance measures. It is finally noted that both the DFN model and Channel Network model applications show a lower level of ergodicity for the *F*-quotient than for travel time in comparison to those of the SC application. This suggests that a spatially variable

flow-wetted surface may result in more non-ergodic conditions.

5. Discussion and conclusions

The AMP study fixes a number of modelling premises, including the modelling domain, boundary conditions, repository layout, and definition of some parameters, in an attempt to create a constrained, useful comparison of the alternative modelling approaches. These restrictions result in model applications, that are similar in most respects, including similar discharge locations and median performance measures. This consistency suggests that the conceptual uncertainties of groundwater flow in fractured rocks have little impact on the expected results of the groundwater flow process model. Since the only flow model results used for subsequent SR 97 performance assessment calculations are canister flux, advective travel time and *F*-quotient along flowpaths, the AMP study results also suggest that this conceptual uncertainty has little impact on the expected repository performance. However, if full distributions of groundwater flow model results are used for subsequent radionuclide transport calculations rather than e.g. median values alone, it appears possible that the expected repository performance will be affected by the inclusion of a spatially variable flow-wetted surface. This is indicated by the large spread of the *F*-quotient distribution of the DFN application relative to the spread of its advective travel time distribution.

The SC results appear to have the highest variability of all three approaches examined, with wider ranges than the other approaches for the ensemble statistics of travel time and canister flux. The relatively small variability of travel time and *F*-quotient of the Channel Network application may be due to the averaging technique used in compiling its results. However, the Channel Network study results have the lowest canister flux variance, indicating that this Channel Network application simply has a lower inferred spatial variability. From a performance assessment point of view, there is limited impact of conceptual model uncertainty implied by using the SC approach alone for obtaining these two output entities for subsequent radionuclide transport calculations. With respect to the *F*-quotient results, the effect of a spatially variable flow-wetted surface suggests that performance assessments may be impacted by uncertainty of this feature of groundwater flow and transport in fractured rocks. A strategy for repository performance assessment thus might reasonably include the use of SC models for analysing groundwater flow at both regional and site scales, and the use of DFN models for obtaining transport related parameters (*F*-quotient) at the site scale or repository scale. To successfully adopt this approach for future applications, it appears instrumental to resolve the discrepancy between the DFN boundary fluxes and those of the regional SC model.

Some of the differences seen between the various models are not only due to pure conceptual differences, but also to differences in modelling strategy and the compilation of performance measure statistics. Examples include the interpretation of underlying hydraulic conductivity data, the representation of the tunnels and disturbed zone in the models, the number of canisters included in the analysis, and the number of realisations. The study has not examined other differences that may exist (e.g. the effects of sample size on parameter inference or the impact of modelling team experience).

Acknowledgements

We would like to thank all the modellers participating in the AMP for their dedicated work and their comments, which have contributed greatly to this paper. We are grateful to P. Mazurek and an anonymous reviewer, whose comments substantially improved the presentation of this study. This paper has benefited from comments and discussions during a seminar hosted by Dr Masahiro Uchida and Dr Atsushi Sawada of the Japan Nuclear Cycle Development Institute. This study was funded by the Swedish Nuclear Fuel and Waste Management Company (SKB).

Appendix A

Tables A1 and A2 provides the full listing of the performance measure statistics for the AMP.

Table A1
Ensemble results (estimates were compiled over all realisations and canisters)

	Stochastic continuum	Channel network	Discrete fracture network
A. log_{10} travel time (*yr*)			
Mean	1.407	1.025	1.453
Variance	0.690	0.193	0.304
Median	1.429	1.033	1.431
5th percentile	−0.013	0.238	0.592
95th percentile	2.766	1.667	2.362
$D = P_{95} - P_5$	2.779	1.429	1.771
B. log_{10} F-quotient (*yr/m*)			
Mean	5.497	4.831	6.195
Variance	0.690	0.216	0.536
Median	5.519	4.869	6.230
5th percentile	4.077	3.948	5.065
95th percentile	6.856	5.404	7.483
$D = P_{95} - P_5$	2.779	1.456	2.417
C. log_{10} canister flux (*m/yr*)			
Mean	−3.190	−3.133	−2.595
Variance	1.116	0.468	0.691
Median	−3.180	−3.260	−2.529
5th percentile	−4.959	−4.017	−4.066
95th percentile	−1.456	−1.654	−1.374
$D = P_{95} - P_5$	3.503	2.363	2.692

Table A2
Variability between realisations (estimates were compiled over all canisters for each realisation, then averaged over all realisations)

	Stochastic continuum	Channel network	Discrete fracture network
A. log_{10} travel time (*yr*)			
Variance of mean var$[\bar{Y}]$	0.019	4.40×10^{-4}	0.272
Variance of variance var$[\sigma_Y^2]$	0.016	3.89×10^{-4}	0.009
Uncertainty in median $UY_{50} = (Y_{50})_{95\%} - (Y_{50})_{5\%}$	0.578	0.084	1.646
Uncertainty of spread $UD_Y = (D_Y)_{95\%} - (D_Y)_{5\%}$	0.980	0.159	0.813
B. log_{10} F-quotient (*yr/m*)			
Variance of mean var$[\bar{Y}]$	0.019	5.89×10^{-4}	0.689
Variance of variance var$[\sigma_Y^2]$	0.016	7.71×10^{-4}	0.065
Uncertainty in median $UY_{50} = (Y_{50})_{95\%} - (Y_{50})_{5\%}$	0.578	0.103	2.374
Uncertainty of spread $UD_Y = (D_Y)_{95\%} - (D_Y)_{5\%}$	0.980	0.314	1.278
C. log_{10} canister flux (*m/yr*)			
Variance of mean var$[\bar{Y}]$	0.022	1.00×10^{-3}	0.491
Variance of variance var$[\sigma_Y^2]$	0.025	1.09×10^{-3}	0.040
Uncertainty in median $UY_{50} = (Y_{50})_{95\%} - (Y_{50})_{5\%}$	0.594	0.123	2.203
Uncertainty of spread $UD_Y = (D_Y)_{95\%} - (D_Y)_{5\%}$	0.960	0.338	1.238

References

Andersson, J., Hermanson, J., Elert, M., Gylling, B., Moreno, L., Selroos, J.-O., 1998. Derivation and treatment of the flow wetted surface and other geosphere parameters in the transport models FARF31 and COMP23 for use in safety assessment, SKB Report R-98-60. Swedish Nuclear Fuel and Waste Management Co., Stockholm, Sweden.

Dershowitz, W., Geier, J., Lee, K., 1989. Field validation of conceptual models for fracture geometry. Submitted for publication.

Dershowitz, W., Thomas, A., Busse, R., 1996. Discrete fracture analysis in support of the Äspö tracer retention understanding experiment (TRUE-1), SKB International Cooperation Report ICR-96-05. Swedish Nuclear Fuel and Waste Management Co., Stockholm, Sweden.

Dershowitz, W., Follin, S., Eiben, T., Andersson, J., 1999. SR 97—alternative models project: discrete fracture network modelling for performance assessment of Aberg, SKB Report R-99-43. Swedish Nuclear Fuel and Waste Management Co., Stockholm, Sweden.

Walker, D., Eriksson, L., Lovius, L. (Eds.), 1996. Analysis of the Äspö LPT2 pumping test via simulation and inverse modelling with HYDRASTAR, SKB Technical Report TR 96-23. Swedish Nuclear Fuel and Waste Management Co., Stockholm, Sweden.

Follin, S., Hermanson, J., 1996. A discrete fracture network model of the Äspö TBM tunnel rock mass, SKB Working Report AR D-97-001. Swedish Nuclear Fuel and Waste Management Co., Stockholm, Sweden.

Gylling, B., 1997. Development and applications of the channel network model for simulations of flow and solute transport in fractured rock. PhD Thesis, Royal Institute of Technology, Stockholm, Sweden.

Gylling, B., Moreno, L., Neretnieks, I., Birgersson, L., 1994. Analysis of LPT2 using the channel network model, SKB International Cooperation Report ICR 94-05. Swedish Nuclear Fuel and Waste Management Co., Stockholm, Sweden.

Gylling, B., Birgersson, L., Moreno, L., Neretnieks, I., 1998. Analysis of a long-term pumping and tracer test using the channel network model. J. Contam. Hydrol. 32, 203–222.

Gylling, B., Moreno, L., Neretnieks, I., 1999a. SR 97—alternative models project: channel network modelling of Aberg: performance assessment using CHAN3D, SKB Report R-99-44. Swedish Nuclear Fuel and Waste Management Co., Stockholm, Sweden.

Gylling, B., Moreno, L., Neretnieks, I., 1999b. The channel network model—a tool for transport simulations in fractured media. Ground Water 37 (3), 367–375.

Moreno, L., Neretnieks, I., 1993. Fluid flow and solute transport in a network of channels. J. Contam. Hydrol. 14 (2), 163–192.

Moreno, L., Gylling, B., Neretnieks, I., 1997. Solute transport in fractured media-the important mechanisms for performance assessment. J. Contam. Hydrol. 25, 283–298.

Munier, R., Sandstedt, H., Niland, L., 1997. Förslag till principiella utformningar av förvar enligt KBS-3 för Aberg, Beberg och Ceberg, SKB Report R-97-09. Swedish Nuclear Fuel and Waste Management Co., Stockholm, Sweden.

Neretnieks, I., 1993. Solute transport in fractured rock—applications to radionuclide waste repositories. In: Bear, J., Tsang, C.-F., de Marsily, G. (Eds.). Flow and Contaminant Transport in Fractured Rock. Academic Press, New York.

Neuman, S., 1988. A proposed conceptual framework and methodology for investigating flow and transport in Swedish crystalline rocks, SKB Working Report AR 88-37. Swedish Nuclear Fuel and Waste Management Co., Stockholm, Sweden.

Neuman, S.P., Jacobsen, E.A., 1984. Analysis of nonintrinsic spatial variability by residual kriging with application to regional groundwater levels. Math. Geol. 15 (5).

Norman, S., 1992. HYDRASTAR—a code for stochastic simulation of groundwater flow, SKB Technical Report TR 92-12. Swedish Nuclear Fuel and Waste Management Co., Stockholm, Sweden.

Rhén, I., Gustafson, G., Stanfors, R., Wikberg, P., 1997. Äspö hard rock laboratory-geoscientific evaluation 1997/5 models based on site characterisation 1986–1995, SKB Technical Report TR 97-06. Swedish Nuclear Fuel and Waste Management Co., Stockholm, Sweden.

Skaguis, K., Wibourgh, M., Ström, A., Morén, L., 1996. Performance assessment of the geosphere barrier of a deep geological repository for spent fuel. ENS TOPSEAL '96 Transactions, Poster Papers vol. II, pp. 141–147.

SKB, 1992. SKB 91: Final disposal of spent nuclear fuel, importance of bedrock for safety, SKB Technical Report TR 92-20. Swedish Nuclear Fuel and Waste Management Co., Stockholm, Sweden.

SKB, 1999. SR 97—post-closure safety: main report summary, SKB Technical Report TR-99-06. Swedish Nuclear Fuel and Waste Management Co., Stockholm, Sweden.

SKI, 1997. SKI site-94 deep repository performance assessment project, Swedish Nuclear Power Inspectorate, SKI Report 97:5, Stockholm, Sweden.

Svensson, U., 1997. A regional analysis of groundwater flow and salinity distribution in the Äspö area, SKB Technical Report TR 97-09. Swedish Nuclear Fuel and Waste Management Co., Stockholm, Sweden.

Uchida, M., Geier, J., 1992. Fracture mapping on Äspö Island, SKB SICADA Database. Swedish Nuclear Fuel and Waste Management Co., Stockholm, Sweden.

Uchida, M., Doe, T., Dershowitz, W., Thomas, A., Wallmann, P., Sawada, A., 1994. Discrete-fracture modeling of the Äspö LPT-2, large-scale pumping and tracer test, SKB International Cooperation Report ICR 94-09. Swedish Nuclear Fuel and Waste Management Co., Stockholm, Sweden.

Uchida, M., Doe, T., Sawada, A., Dershowitz, W., Wallmann, P., 1997. FracMan discrete fracture modeling for the Äspö tunnel drawdown experiment, SKB International Cooperation Report ICR 97-03. Swedish Nuclear Fuel and Waste Management Co., Stockholm, Sweden.

Walker, D., Gylling, B., Ström, A., Selroos, J.-O., 2001. Hydrogeologic studies for nuclear waste disposal in Sweden. Hydrogeol. J. 9 (5).

Ward, D., Buss, D., Mercer, J., Hughes, S., 1987. Evaluation of a groundwater corrective action at the Chem-Dyne hazardous waste site using a telescopic mesh refinement modelling approach. Water Resour. Res. 23 (4), 603–617.

Widén, H., Walker, D., 1999. SR 97—alternative models project: stochastic continuum modelling of Aberg, SKB Report R-99-42. Swedish Nuclear Fuel and Waste Management Co., Stockholm, Sweden.